RPE | Radiation Physics & Engineering
A Peer-Reviewed Journal
Published by K.N. Toosi University of Technology
http://rpe.kntu.ac.ir
Research Article

Radiation Physics and Engineering 2025; 6(3):49–54

Low-cost active detectors for radon gas detection: some preliminary test results

Ehsan Parsazadeh, Kamal Hadad, Mohammad-Reza Mohammadian-Behbahani*, Ahmad Pirouzmand

Department of Nuclear Engineering, School of Mechanical Engineering, Shiraz University, Shiraz, Iran

HIGHLIGHTS

- The study evaluates low-cost active detectors for Radon gas monitoring.
- Three different detectors are studied.
- The three detectors exhibit either an increasing or decreasing response as the concentration of Radon gas changes.

ABSTRACT

Radon gas is a significant source of natural radiation exposure in humans. In this research, the responses of three different radiation detectors are compared by preliminary test results for Radon gas detection. First detector is a pulse-mode counter developed by using a BPW34 photodiode. To amplify and read out the output signal of the photodiode, a charge-sensitive preamplifier, based on a two-stage TLC272 operational amplifier is designed. In the following, a pulse counting circuit is implemented by using an ATmega32 microcontroller. The second developed detector is a current-mode air ionization chamber working at low applied voltages, with output signal enhanced by a current amplifier BC517 Darlington transistor, read out by an Arduino UNO module. Additionally, an alpha-sensitive Geiger-Mueller counter (model NT-960, Novin Teyf) with a mica entrance window is employed as the third detector. Soil samples containing natural Uranium, in companion with all three detectors were sealed in a chamber to study the detector responses to different concentrations of Radon gas. Findings indicate that all three detectors exhibit an increasing response as the concentration of Radon gas is increased. In the viewpoint of measurement accuracy, the Geiger-Mueller counter provides more accurate results due to a higher count rate and lower statistical fluctuations, with a concentration curve giving the half-life of Radon acceptably. The ionization chamber is shown to suffer from low sensitivity due to its current-mode operation.

KEYWORDS

Arduino-based ion chamber
Geiger-Mueller counter
Photodiode detector
Radon gas monitoring

HISTORY

Received: 23 August 2024
Revised: 13 December 2024
Accepted: 24 February 2025
Published: Summer 2025

1 Introduction

Radon-222 is a noble gas originating from the radioactive decay chain of Uranium or Thorium, both of which found in minimal quantities in rocks and soils. The concentration of Radon gas varies by geographical region and environmental conditions. Radon-222 undergoes alpha decay with a half-life of 3.82 days, leading to the formation of Polonium-218, which subsequently decays to Lead-214 through alpha decay with a half-life of 3.10 minutes. Alpha particles, having a high linear energy transfer, can inflict serious damage to cells along their path within tissue.

The World Nuclear Association currently identifies Radon as the main reason for radiation exposure in humans. Its invisibility, lack of odor, taste, and color make it difficult to identify without specific tools. Although Radon detectors are commercially available, their affordability may restrict their access. Passive detectors and electret systems are commonly used for long-term measurements of Radon, while systems with continuous function are most often used for online short-term measurements (Sukanya and Joseph, 2023; Ishimori et al., 2013; Ćujić et al., 2021; Organization, 2009; United, 1982; Blanco-Novoa et al., 2018; Mishra et al., 2009).

Radon and its decay products may emit alpha particles, beta particles or gamma rays. Hence, a variety of alpha, beta, and gamma detectors can be applied: solid and liquid scintillation detectors, nuclear track detectors, electrometers, ionization chambers, semiconductor detec-

*Corresponding author: m.mohammadian@saadi.shirazu.ac.ir

https://doi.org/10.22034/rpe.2025.474882.1237

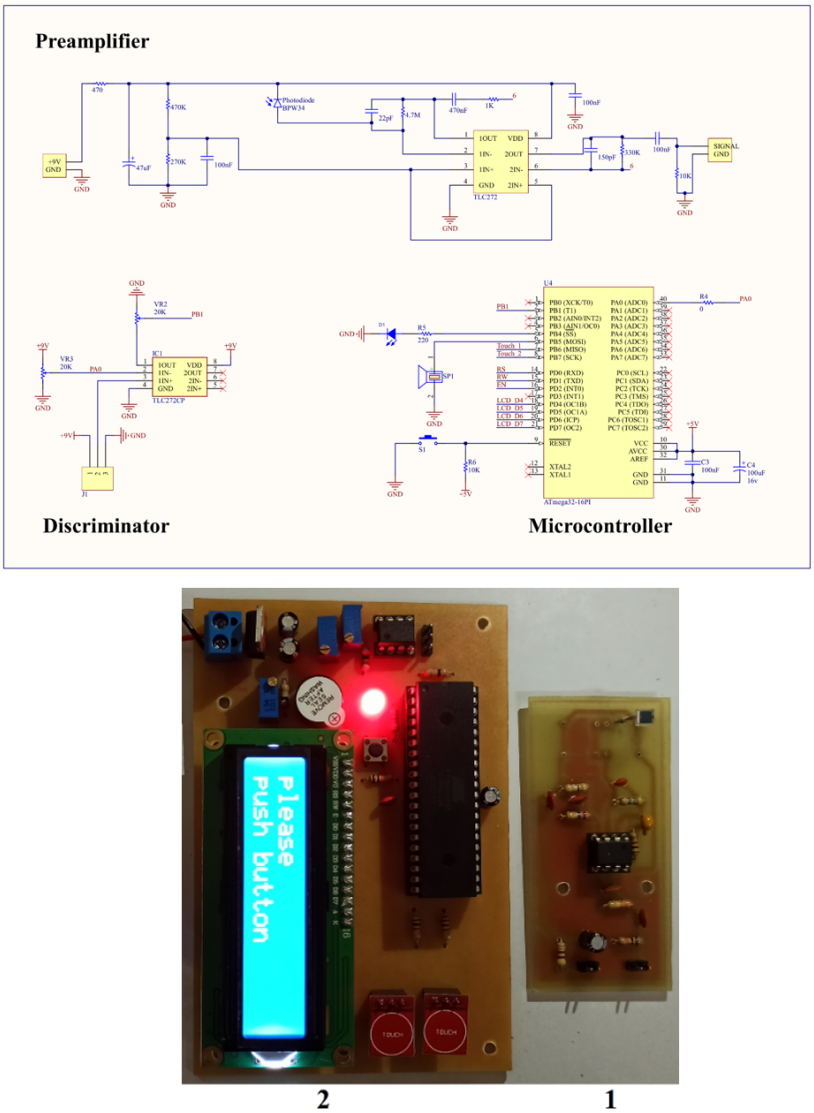

Figure 1: The photodiode detector. Top: schematic view of the detector designed in Altium Designer software. Down: assembled detector, including (1) the charge-sensitive preamplifier with the BPW34 photodiode, and (2) the counter system.

tors, and thermo-luminescence detectors (Budnitz, 1974).

Elisio and Peralta utilized a SLCD-61N5 low-cost planar photodiode and a charge-sensitive preamplifier, along with an Arduino-based counter system, as an active Radon gas detector (Elísio and Peralta, 2020). Blanco-Novoa et al. tested an IoT remote Radon monitoring system for accurate measurement of Radon concentration in various locations including buildings in Galicia, Spain, where high levels of Radon gas are expected (Blanco-Novoa et al., 2018). Kim et al. studied a PIN photodiode Radon sensor by which the measured rate for Radon-emitting soil was 4.38 counts per hour (Kim et al., 2016). Bayrak et al. utilized a low-cost Radon detection system for predicting earthquakes, made of a windowless PS100-7-CER-2 photodiode, in companion with an amplifier and shaper (Bayrak et al., 2013).

Brizova et al. studied an ionization chamber in current-mode to detect alpha particles, equipped with an Arduino module (Břízová et al., 2020). Studnicka et al. tested a low-cost current-mode ion chamber developed for monitoring Radon gas, operating at a low voltage. Their study reported a minimum measurable activity of approximately 50 Bq.m^{-3} for Radon gas (Studnička et al., 2019).

In the current study, we mainly aim to assess the performance of two detectors: a pulse-mode detector based on a photodiode, and a current-mode ionization chamber. Results by an alpha-sensitive Geiger-Mueller counter are also reported for comparison.

2 Experimental set up

In this research, two detectors similar to (Studnička et al., 2019) and https://stoppi-homemade-physics.de/alphaspektroskopie/ were developed: a photodiode detector and a free air ionization chamber (Figs. 1 and 2, respectively). Additionally, a Novin Teyf NT-960 Geiger-Mueller counter (https://www.novinteyf.ir/nt-960) was used. This detector, with a thin mica entrance window, is sensitive to alpha particles. A commercial Geiger-Muller detector incurs much higher costs

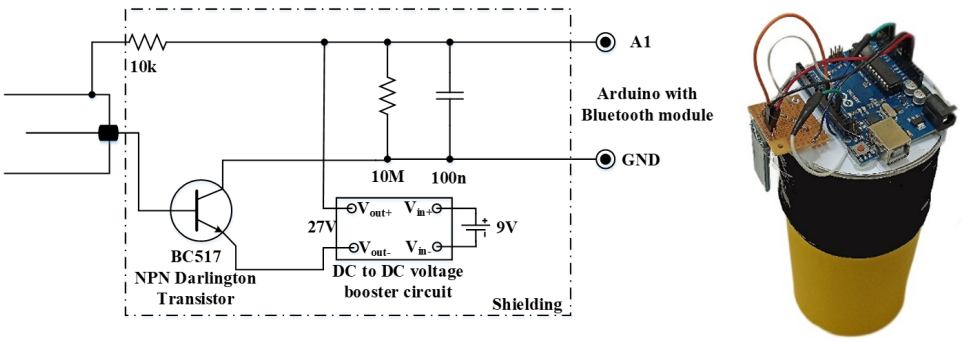

Figure 2: The current-mode ionization chamber: Left: the detector sensor circuit. Right: the fabricated detector.

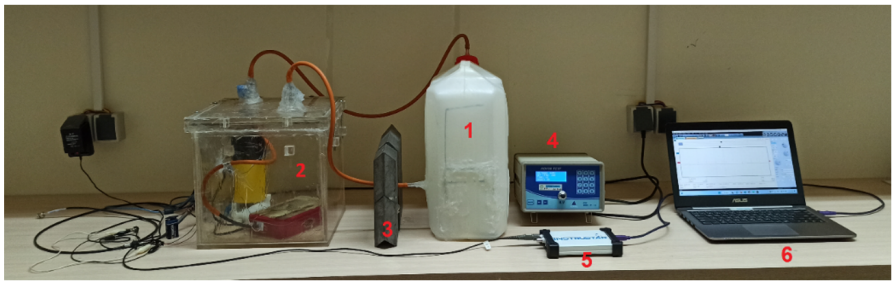

Figure 3: The experimental setup. (1) An insulated container of Uranium ore and soil which produce Radon gas. (2) An insulated chamber where detectors are placed inside. (3) Lead blocks to protect the detectors from direct exposure by gamma rays from chamber 1. (4) Power supply and readout system of the Geiger-Mueller detector. (5) InstruStar-ISDS205A oscilloscope card. (6) Laptop for reading the output of the oscilloscope card.

than the proposed detection systems, needing a well- designed, aligned and sealed cylindrical geometry, multiplication and quenching mechanisms, and high-voltage system. The photodiode detector, on the other hand, requires some generic electronic components, working under the bias of a 9 V battery. The ionization chamber is also a low-cost device due to working by free air and no need for a high-voltage system. All these three detectors were placed in a well-insulated chamber.

The output signals of the photodiode were amplified and processed using a charge-sensitive preamplifier. To achieve this, a two-stage TLC272 operational amplifier was utilized. A discriminator unit was also implemented to produce logic pulses that correspond to the particles detected by the photodiode. Finally, an Atmega32 microcontroller was programmed to calculate the rate of logic pulses and display the result on a LCD screen (Parsazadeh et al., 2023) (Fig. 1). To enhance the detection of beta particles, the protective plastic layer on the photodiode was sanded down to a much lower thickness. The BPW34 photodiode (https://www.vishay.com/docs/81521/bpw34.pdf), in companion with the preamplifier were enclosed in a metal casing to protect from interfering light or electromagnetic waves. A tiny hole on the metal box permitted the passage of Radon gas, while blocking the environmental light.

In the ion chamber, a guard ring is employed to minimize the leakage current. A BC517 NPN Darlington transistor (https://static.chipdip.ru/lib/958/DOC003958404.pdf) is used to amplify the chamber current signal (Fig. 2). A DC voltage booster module is employed to enhance the applied voltage. To measure the output signal, the analog-to-digital converter of an Arduino UNO board is utilized. The recorded values are then transmitted to an smartphone via a HC-05 Bluetooth module. To prevent from electromagnetic wave interferences, a metal cap envelopes the readout circuit on the top, and a metal grid covers the bottom side of the chamber, where the radiations are allowed to enter via.

The experimental setup is shown in Fig. 3, in which there exist two separate chambers: one containing Uranium soil (1) and the other, the detectors (2). The total volume of these chambers is roughly 40 liters. During the measurements, the room temperature was held at 25 °C. An InstruStar-ISDS205A oscilloscope card was utilized to monitor the outputs of the detectors.

3 Results and discussion

Figure 4 indicates the settings and output data of the Geiger-Mueller detector, with counting results arbitrarily for day 10 of the experiment. The applied voltage is 450 V, measurement time 100 s and the recorded count 187. Measurements were repeated multiple time each day and the results averaged and the corresponding standard deviation calculated.

Figure 5 illustrates three output pulses captured by the oscilloscope card from the photodiode detector on day 15 of the experiment. To reject the background noise signals, a threshold level of 20 mV was set for the discriminator circuit.

Figure 4: Setup and measured count with the Geiger-Muller detector on day 10 of the experiment.

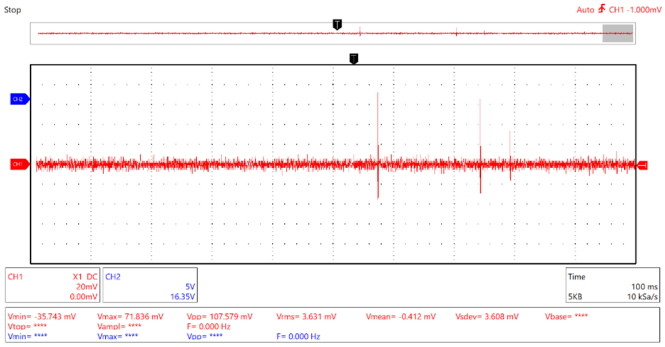

Figure 5: Some photodiode detector output pulses recorded on day 15.

Figures 6-a, 6-b and 6-c respectively illustrated the output currents of the ion chamber, recorded by the InstruStar-ISDS205A oscilloscope card, arbitrarily on day 0 (before the introduction of Radon gas, representing the detector leakage current) day 11 and day 15. As the Radon concentration increases, the absolute value of the recorded average current is also increased: 25.36 ± 9.89, 57.33 ± 7.84, and 87.89 ± 6.29 mV as in Figs. 6-a, 6-b and 6-c, respectively.

Curves of the measured concentrations of Radon by the three detectors are presented in Fig. 7. First to measure the background/leakage values, the Geiger-Mueller detector, the ion chamber, and the photodiode detector were set up in the absence of Radon gas, and their corresponding values recorded (shown as the data points of day 0 in Fig. 7). The count rates of the Geiger-Mueller and the photodiode detectors were obtained by averaging the counts recorded over 100-second intervals of data acquisition.

Subsequently, the Radon gas was introduced, allowed to enter the chamber for 15 days, which corresponds to roughly four half-lives of Radon. During this period, the Radon concentration built up. In the next phase, the entrance valve was closed so as to evaluate the decrease in Radon concentration. Measured values of each detector were normalized to their corresponding maximum value (reached on day 15), and the concentration curves plotted altogether in Fig. 7.

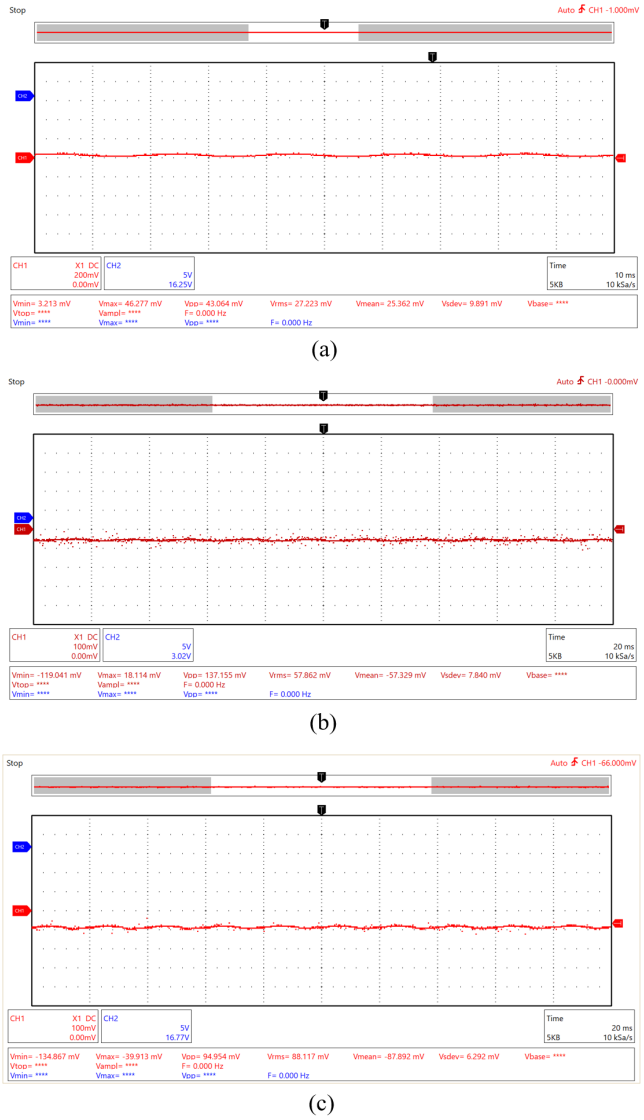

Figure 6: Examples of the ionization chamber detector output currents recorded on days 0 (a), 11 (b) and 15 (c). Negative values for the currents is associated with the polarity of the probe connection.

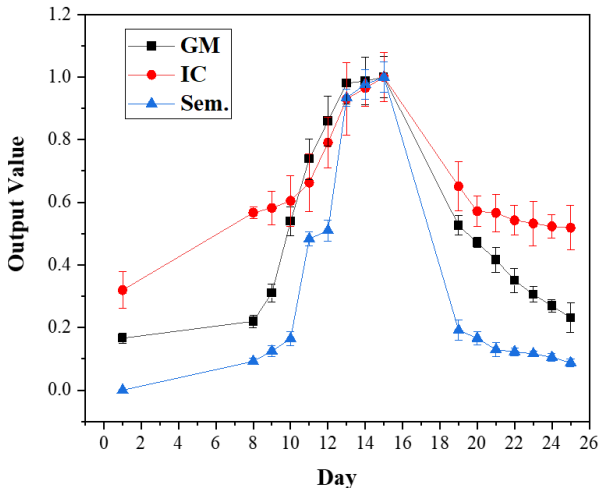

Figure 7: Normalized concentration curves of the three detectors: the Geiger-Mueller (GM) detector, ion chamber (IC) and the semiconductor photodiode detector (Sem.). The Radon entrance valve was closed on day 15.

An exponential fitting of the decaying part of the GM curve in Fig. 7 gives the half-life ($t_{1/2}$) of Radon gas acceptably. To this goal, a single exponential function as Eq. (1) was fitted to the data points of days 15-25 of the GM curve.

$$y(t) = y_0 + A\,\mathrm{e}^{-0.693(t-t_0)/t_{1/2}} \quad (1)$$

where y_0 is a bias term, A amplitude, t time in days and $t_0 = 15$ the start time. The fitting result gives a calculated $t_{1/2}$ of 4.2 days, in acceptable accordance with the true half-life of Radon, 3.82 days. The discrepancy may be attributed to the absence of information on days without measurement, as well as the measurement errors.

While the Geiger-Mueller counter acceptably follows the expected behavior, the photodiode detector fails due to its quite lower number of counts (due to its lower detection efficiency) and increased statistical fluctuations of the recorded counts. A lower sensitivity for the photodiode detector is also observed with outputs tending to zero when the activity is low (after day 18 and before day 8). For the case of ion chamber, a relatively large background leakage current (the normalized output level of nearly 0.5 in Fig. 7) is observed from which the curve rises and to which it returns back. This high level of leakage current limits the sensitivity of the ion chamber. Despite the fact that the results by the ion chamber and the photodiode detector deviate from expectations, in general, it can be observed that when the concentration of Radon gas inside the chamber was increased, all three detectors exhibited an increasing trend of their outputs. Conversely, when the gas valve was closed and the concentration of Radon decreased, all three detectors recorded a decreasing trend of data.

4 Conclusions

In this study, the design and preliminary test results of two low-cost detectors, a photodiode detector and an ion chamber, were reported. These detectors benefit from several advantages including portability, compactness, online response (in comparison with the passive Radon detectors), low energy consumption and low manufacturing costs. Generally based on experimental tests, it was shown that both detectors, along with a standard Geiger-Mueller counter, could follow the increasing and decreasing trends in Radon gas concentration. Our group aims to work further on the limitations of the proposed detectors, which include their sensitivity and probable response stability issues.

Acknowledgements

The authors would like to express their gratitude to the Radiation Research Center of Shiraz University for supplying the radioactive sources and facilitating the test conditions. They also wish to thank Mosayeb Dehghani, the laboratory staff at the School of Mechanical Engineering, Shiraz University for his technical assistance.

Conflict of Interest

The authors declare no potential conflict of interest regarding the publication of this work.

References

Bayrak, A., Barlas, E., Emirhan, E., et al. (2013). A complete low cost radon detection system. *Applied Radiation and Isotopes*, 78:1–9.

Blanco-Novoa, O., Fernández-Caramés, T. M., Fraga-Lamas, P., et al. (2018). A cost-effective iot system for monitoring indoor radon gas concentration. *Sensors*, 18(7):2198.

Břízová, L., Šlégr, J., and Váňová, K. (2020). Simple alpha particle detector with an air ionization chamber. *The Physics Teacher*, 58(1):42–45.

Budnitz, R. J. (1974). Radon-222 and its daughters-A review of instrumentation for occupational and environmental monitoring. *Health Physics*, 26(2):145–163.

Ćujić, M., Janković Mandić, L., Petrović, J., and Dragović, R. o. (2021). Radon-222: environmental behavior and impact to (human and non-human) biota. *International Journal of Biometeorology*, 65:69–83.

Elísio, S. and Peralta, L. (2020). Development of a low-cost monitor for radon detection in air. *Nuclear Instruments and Methods in Physics Research Section A: Accelerators, Spectrometers, Detectors and Associated Equipment*, 969:164033.

Ishimori, Y., Lange, K., Martin, P., et al. (2013). Measurement and calculation of radon releases from NORM residues.

Kim, G.-S., Oh, T.-G., and Kim, J.-H. (2016). Implementation of a PIN photodiode radon counter. *Global Journal of Engineering Science and Researches*, 3(1):58–63.

Mishra, R., Sapra, B., and Mayya, Y. (2009). Development of an integrated sampler based on direct ^{222}Rn/^{220}Rn progeny sensors in flow-mode for estimating unattached/attached progeny concentration. *Nuclear Instruments and Methods in Physics Research Section B: Beam Interactions with Materials and Atoms*, 267(21-22):3574–3579.

Organization, W. H. (2009). *WHO handbook on indoor radon: a public health perspective*. World Health Organization.

Parsazadeh, E., Hadad, K., Mohammadian-Behbahani, M. R., et al. (2023). Design and construction of a beta ray detector using BPW34 photodiode (In Persian). *29th National Conference on Nuclear Science and Technology, Tehran, Iran*.

Studnička, F., Štěpán, J., and Šlégr, J. (2019). Low-cost radon detector with low-voltage air-ionization chamber. *Sensors*, 19(17):3721.

Sukanya, S. and Joseph, S. (2023). *Environmental radon: a tracer for hydrological studies*. Springer Nature.

United, N. (1982). Ionizing radiation: sources and biological effects. *UNSCEAR report*.

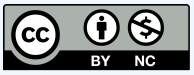

To cite this article:

Parsazadeh, E. , Hadad, K. , Mohammadian Behbahani, M. and Pirouzmand, A. (2025). Low-cost active detectors for radon gas detection: some preliminary test results. *Radiation Physics and Engineering*, 6(3), 49-54. doi: 10.22034/rpe.2025.474882.1237

DOI: 10.22034/rpe.2025.474882.1237

To link to this article: https://doi.org/10.22034/rpe.2025.474882.1237